Inorg. Chem. **2009**, *48*, 1989−2000

Design Considerations for a System for Photocatalytic Hydrogen Production from Water Employing Mixed-Metal Photochemical Molecular Devices for Photoinitiated Electron Collection

Shamindri M. Arachchige, Jared R. Brown, Eric Chang, Avijita Jain, David F. Zigler, Krishnan Rangan, and Karen J. Brewer*

Department of Chemistry, Virginia Polytechnic Institute and State University, Blacksburg, Virginia 24061-0212

Received September 9, 2008

Supramolecular complexes coupling Ru(II) or Os(II) polyazine light absorbers through bridging ligands to Rh(III) or Ir(III) allow the study of factors impacting photoinitiated electron collection and multielectron water reduction to produce hydrogen. The $[\{(bpy)_2Ru(dpb)\}_2IrCl_2](PF_6)_5$ system represents the first photoinitiated electron collector in a molecular system (bpy = 2,2′-bipyridine, dpb = 2,3-bis(2-pyridyl)benzoquinoxaline). The $[\{(bpy)_2Ru(dpp)\}_2RhCl_2](PF_6)_5$ system represents the first photoinitiated electron collector that affords photochemical hydrogen production from water in the presence of an electron donor, *N,N*-dimethylaniline (dpp = 2,3-bis(2-pyridyl)pyrazine). The complexes $[\{(bpy)_2Ru(dpp)\}_2RhCl_2](PF_6)_5$, $[\{(bpy)_2Ru(dpp)\}_2RhBr_2](PF_6)_5$, $[\{(phen)_2Ru(dpp)\}_2RhCl_2](PF_6)_5$, $[\{(bpy)_2Os(dpp)\}_2RhCl_2](PF_6)_5$, $[\{(tpy)RuCl(dpp)\}_2RhCl_2](PF_6)_3$, $[\{(tpy)OsCl(dpp)\}_2RhCl_2](PF_6)_3$, and $[\{(bpy)_2Ru(dpb)\}_2IrCl_2](PF_6)_5$ are herein evaluated with respect to their functioning as hydrogen photocatalysts (tpy = 2,2′:6′,2″-terpyridine, phen = 1,10-phenanthroline). With the exceptions of $[\{(bpy)_2Ru(dpb)\}_2IrCl_2](PF_6)_5$ and $[\{(tpy)OsCl(dpp)\}_2RhCl_2](PF_6)_3$, all other complexes demonstrate photocatalytic activity. The functioning systems possess a rhodium localized lowest unoccupied molecular orbital that serves as the site of electron collection and a metal-to-ligand charge-transfer (^{3}MLCT) and/or metal-to-metal charge-transfer (^{3}MMCT) excited-state with sufficient driving force for excited-state reduction by the electron donor. The lack of photocatalytic activity by $[\{(bpy)_2Ru(dpb)\}_2IrCl_2](PF_6)_5$, although photoinitiated electron collection occurs, establishes the significance of the rhodium center in the photocatalytic system. The lack of photocatalytic activity of $[\{(tpy)OsCl(dpp)\}_2RhCl_2](PF_6)_3$ is attributed to the lower-energy ^{3}MLCT state that does not possess sufficient driving force for excited-state reduction by the electron donor. The variation of electron donor showed the photocatalysis efficiency to decrease in the order *N,N*-dimethylaniline > triethylamine > triethanolamine. The general design considerations for development of supramolecular assemblies that function as water reduction photocatalysts are discussed.

Introduction

The development of a clean renewable energy source has been a worldwide goal for more than 30 years. Developing the technology to utilize renewable resources is especially important today with depleting oil reserves. Considerable research has focused on light-to-energy conversion with efficient hydrogen production from water an important goal.[1−6] The discovery of $[Ru(bpy)_3]^{2+}$ (bpy = 2,2′-bipyridine), which possesses a long-lived metal-to-ligand charge-transfer (MLCT) excited state, has inspired photochemical and photophysical studies of similar polyazine complexes being applied to light-to-energy conversion research.[7−9] The

* To whom correspondence should be addressed. E-mail: kbrewer@vt.edu.

(1) Willner, I.; Willner, B. *Top. Curr. Chem.* **1991**, *159*, 153.
(2) Koelle, U. *New J. Chem.* **1992**, *16*, 157.
(3) Amouyal, E. *Sol. Energy Mater. Sol. Cells* **1995**, *38*, 249.
(4) Bard, A. J.; Fox, M. A. *Acc. Chem. Res.* **1995**, *28*, 141.
(5) Bolton, J. R. *Sol. Energy* **1996**, *57*, 37.
(6) Esswein, A. J.; Nocera, D. G. *Chem. Rev.* **2007**, *107*, 4022.
(7) Kalyanasundaram, K. *Coord. Chem. Rev.* **1982**, *46*, 159.
(8) Juris, A.; Balzani, V.; Barigelletti, F.; Campagna, S.; Belser, P.; von Zelewsky, A. *Coord. Chem. Rev.* **1988**, *84*, 85.
(9) Balzani, V.; Moggi, L.; Scandola, F. In *Supramolecular Photochemistry*; Balzani, V., Ed.; NATO ASI Series 214, Reidel, Dordrecht: The Netherlands, 1987, 1, and references therein.

10.1021/ic8017387 CCC: $40.75
Published on Web 02/04/2009

complex $[Ru(bpy)_3]^{2+}$ and other light-absorbing analogues possess ^{3}MLCT states of sufficient energies to split water into hydrogen and oxygen, yet direct photocatalysis does not occur. The overall reaction for water splitting and the related half-reactions are represented in eqs 1−3 at pH 7 versus NHE.[10]

$$2H_2O \rightarrow 2H_2 + O_2 \qquad E = -1.23\ V \qquad (1)$$

$$4H^+ + 4e^- \rightarrow 2H_2 \qquad E = -0.41\ V \qquad (2)$$

$$2H_2O \rightarrow O_2 + 4H^+ + 4e^- \qquad E = -0.82\ V \qquad (3)$$

The energy requirements for water splitting through multielectron processes is much less (1.23 V)[4,10] than through single-electron processes (~5 V)[10] requiring the development of systems to deliver the multiple reducing equivalents. Complicated multicomponent systems incorporating light absorbing (LA) units, electron relays, and redox catalysts have been extensively utilized in solar energy conversion schemes.[1,3,6]

Systems using rhodium complexes in photochemical hydrogen production are known. Tris(polyazine)rhodium(III) complexes serve as electron acceptors in intermolecular schemes. Lehn and Sauvage[10] and Creutz and Sutin[11] have studied a four-component system for hydrogen production using a $[Ru(bpy)_3]^{2+}$ LA, $[Rh(bpy)_3]^{3+}$ electron relay, triethanolamine (TEOA) as a sacrificial electron donor (ED), and a colloidal Pt catalyst. Photolysis results in the transfer of electrons from the excited state of $*[Ru(bpy)_3]^{2+}$ into a Rh(dσ*) acceptor orbital. The newly generated $[Rh^{II}(bpy)_3]^{2+}$ transfers electrons to the Pt colloid, which produces hydrogen in the presence of water. The $[Rh^{II}(bpy)_3]^{2+}$ also disproportionates to $[Rh^{I}(bpy)_2]^+$ and $[Rh^{III}(bpy)_3]^{3+}$. At low concentrations in alkaline solutions, $[Rh^{I}(bpy)_2]^+$ predominates.[12] At higher $[Rh^{I}(bpy)_2]^+$ concentrations a dimer is formed − $[Rh^{I}(bpy)_2]_2^{2+}$. Lowering the pH at low $[Rh^{I}(bpy)_2]^+$ concentration leads to oxidative addition of H_3O^+ affording $[Rh^{III}(bpy)_2(H)(H_2O)]^{2+}$, whereas increasing the $[Rh^{I}(bpy)_2]^+$ concentration affords $[Rh^{I}(bpy)_2]_2(H)^{3+}$.[12] Reversible binding of hydrogen to the $[Rh^{I}(bpy)_2]^+$ complex occurs, and $K_H = 1.45 \times 10^3\ M^{-1}$.[13] It was found that *cis*-$[Rh^{III}(H)_2(bpy)_2]^+$ dissociates to hydrogen and $[Rh^{I}(bpy)_2]^+$ when irradiated ($\lambda > 300$ nm). Petersen studied a series of monometallic rhodium and bimetallic rhodium−ruthenium hydrides of the form $[Rh^{III}(H)_2(PPh_3)_2L]^+$ and $[(bpy)_2Ru^{II}BLRh^{III}(H)_2(PPh_3)_2]^{3+}$ (BL = 2,2′-bipyrimidine (bpm), 2,3-bis(2-pyridyl)pyrazine (dpp), or 2,3-bis(2-pyridyl)quinoxaline (dpq)), which evolve hydrogen upon photolysis $\lambda < 436$ nm.[14] Oishi[15] and Bauer[16] studied the Wilkinson's catalyst analog $[Rh^{I}Cl(dpm)_3]^{3-}$ (dpm = diphenylphosphino-benzene-*m*-sulfonate), which when photolyzed in the presence of $[Ru(bpy)_3]^{2+}$ and ascorbic acid produces hydrogen.

Despite the increasing interest in multielectron photochemical molecular devices, working systems that can effect multielectron reactions remain a challenge. Supramolecular systems coupling LA units to reactive metal centers through bridging ligands (BLs) are of interest in this forum. The supramolecular complexes described are complicated assemblies composed of multiple subunits. Each subunit provides a function that, when combined into the supramolecule, allows for complex functioning of the assemblies.[9] The first functioning photoinitiated electron collector in a molecular system is the $[\{(bpy)_2Ru(dpb)\}_2IrCl_2](PF_6)_5$ system.[17] When excited with visible light in the presence of the electron donor, *N*,*N*-dimethylaniline (DMA), photochemical reduction by two electrons occurs to form $[\{(bpy)_2Ru(dpb^-)\}_2IrCl_2]^{3+}$. This system has not been shown to deliver the photochemically collected electrons to a substrate. MacDonnell and Campagna reported systems that couple two ruthenium LA units through extended aromatic BLs that are of the form $[(phen)_2Ru(BL)Ru(phen)_2]^{4+}$.[18] These complexes function by optical excitation into phen-type orbitals on the BLs followed by electron transfer to lower-lying secondary π*-acceptor orbitals that collects the reducing equivalents with added TEA. Multielectron photocatalysis is not observed, likely due to the collection of the electrons on a remote organic acceptor.

Electron collection on a metal center is also possible. Bocarsly has studied a series of Pt(IV)-centered trimetallic complexes of the form $[(NC)_5M^{II}(CN)Pt^{IV}(NH_3)_4(NC)M^{II}(CN)_5]^{4-}$ (M = Fe, Ru, or Os) that undergo photoinitiated electron collection on metal centers using two Fe, Ru, or Os LAs.[19] Absorption of one photon of light for the complex M = Fe results in a net two-electron transfer to the central Pt(IV) followed by cleavage of the polymetallic complex into two Fe(III) moieties and a reduced Pt(II) monometallic complex. Multielectron photocatalysis is not possible due to complex fragmentation.

Nocera designed metal−metal bonded systems that undergo photochemical multielectron chemistry, which are able to convert hydrohalic acids to hydrogen using light and a halogen trap.[6,20,21] Photolysis of the dirhodium photocatalyst, $[Rh_2^{0,0}(dfpma)_3(PPh_3)(CO)]$ (dfpma = $MeN(PF_2)_2$), results in photolabilization of CO, attack by HCl at both metal

(10) (a) Lehn, J.-M.; Sauvage, J.-P. *Nouv. J. Chim.* **1977**, *1*, 449. (b) Kirch, M.; Lehn, J.-M.; Sauvage, J.-P. *Helv. Chim. Acta* **1979**, *62*, 1345.

(11) (a) Brown, G. M.; Chan, S.-F.; Creutz, C.; Schwarz, H. A.; Sutin, N. *J. Am. Chem. Soc.* **1979**, *101*, 7638. (b) Chan, S.-F.; Chou, M.; Creutz, C.; Matsubara, T.; Sutin, N. *J. Am. Chem. Soc.* **1981**, *103*, 369.

(12) (a) Chou, M.; Creutz, C.; Mahajan, D.; Sutin, N.; Zipp, A. P. *Inorg. Chem.* **1982**, *21*, 3989. (b) Schwarz, H. A.; Creutz, C. *Inorg. Chem.* **1983**, *22*, 707.

(13) (a) Yan, S. G.; Brunschwig, B. S.; Creutz, C.; Fujita, E.; Sutin, N. *J. Am. Chem. Soc.* **1998**, *120*, 10553. (b) Fujita, E.; Brunschwig, B. S.; Creutz, C.; Muckerman, J. T.; Sutin, N.; Szalda, D.; van Eldik, R. *Inorg. Chem.* **2006**, *45*, 1595.

(14) MacQueen, D. B.; Petersen, J. D. *Inorg. Chem.* **1990**, *29*, 2313.

(15) Oishi, S. *J. Mol. Catal.* **1987**, *39*, 225.

(16) Bauer, R.; Werner, H. A. F. *Int. J. Hydrogen Energy* **1994**, *19*, 497.

(17) Molnar, S. M.; Nallas, G.; Bridgewater, J. S.; Brewer, K. J. *J. Am. Chem. Soc.* **1994**, *116*, 5206.

(18) (a) Konduri, R.; Ye, H.; MacDonnell, F. M.; Serroni, S.; Campagna, S.; Rajeshwar, K. *Angew. Chem., Int. Ed.* **2002**, *41*, 3185. (b) Chiorboli, C.; Fracasso, S.; Scandola, F.; Campagna, S.; Serroni, S.; Konduri, R.; MacDonnell, F. M. *Chem. Commun.* **2003**, 1658. (c) Chiorboli, C.; Fracasso, S.; Ravaglia, M.; Scandola, F.; Campagna, S.; Wouters, K. L.; Konduri, R.; MacDonnell, F. M. *Inorg. Chem.* **2005**, *44*, 8368.

(19) (a) Chang, C. C.; Pfennig, B.; Bocarsly, A. B. *Coord. Chem. Rev.* **2000**, *208*, 33. (b) Mordas, C. J.; Pfennig, B. W.; Schreiber, E.; Bocarsly, A. B. *Springer Series in Chem. Phys.* **2003**, *71*, 453. (c) Watson, D. F.; Tan, H. S.; Schreiber, E.; Mordas, C. J.; Bocarsly, A. B. *J. Phys. Chem. A* **2004**, *108*, 3261.

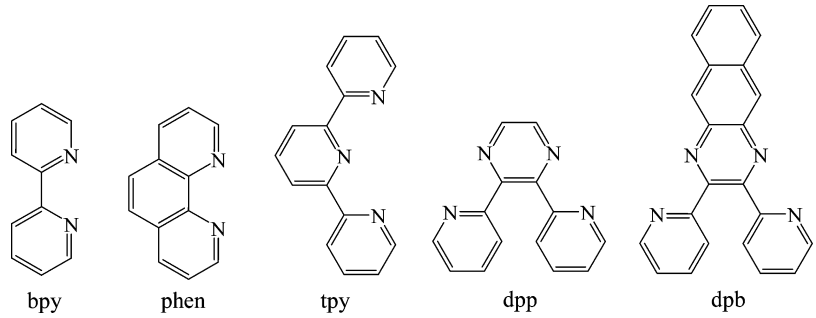

Figure 1. Terminal and bridging ligands employed in the supramolecular complexes investigated. (bpy = 2,2′-bipyridine, phen = 1,10-phenanthroline, tpy = 2,2′:6′,2″-terpyridine, dpp = 2,3-bis(2-pyridyl)pyrazine, dpb = 2,3-bis(2-pyridyl)benzoquinoxaline.)

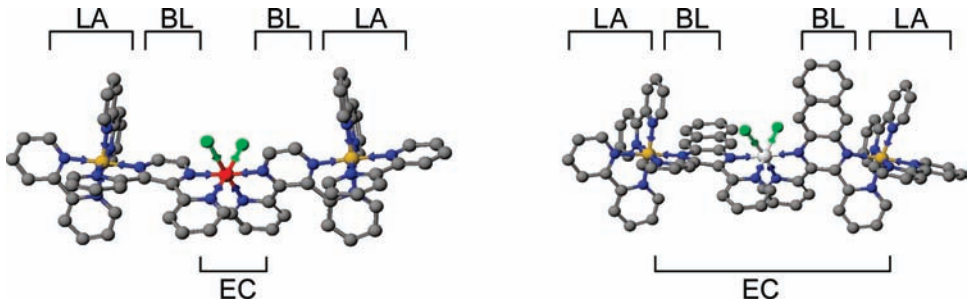

Figure 2. Supramolecular complexes $[\{(bpy)_2Ru(dpp)\}_2RhCl_2]^{5+}$ (left) and $[\{(bpy)_2Ru(dpb)\}_2IrCl_2]^{5+}$ (right) that undergo photoinitiated electron collection (LA = light absorber, BL = bridging ligand, and EC = electron collector; yellow = Ru, red = Rh, white = Ir, gray = C, blue = N, green = Cl). Hydrogen is omitted for clarity.

centers, release of hydrogen, and in the presence of a halogen atom trap regeneration of the catalytically active species $[Rh_2^{0,0}(dfpma)_3L]$ with a hydrogen yield $\Phi \approx 0.01$.

Mixed-metal polyazine complexes have been recently explored that couple ruthenium LAs to reactive metal sites. Sakai recently investigated a $[Pt^{II}(bpy)_2Cl_2]$ component linked to a ruthenium LA through an amide linkage to ruthenium capable of photochemically producing hydrogen from water ($\Phi \approx 0.01$ and 5 turnovers in 10 h) in the presence of ethylenediaminetetraacetic acid.[22] Rau reported a Ru−Pd bimetallic system that photochemically produces hydrogen in the presence of the electron donor, TEA, affording 56 turnovers in ∼30 h.[23] Recent studies by Eisenberg and Castellano on platinum systems[24] and Hammarström on palladium[25] systems suggest hydrogen production can be attributed to decomplexation of the reactive metal to form colloidal metal, which functions as the hydrogen generation site.

Brewer recently reported the photoinitiated electron collection by a metal center in $[\{(bpy)_2Ru(dpp)\}_2RhCl_2](PF_6)_5$.[26] When excited with visible light, this complex is reduced converting the Rh(III) to Rh(I), which undergoes chloride loss to form $[\{(bpy)_2Ru(dpp)\}_2Rh^{I}]^{5+}$.[26] This complex photochemically reduces water to hydrogen using visible light excitation with a $\Phi \approx 0.01$ in the presence of a sacrificial electron donor DMA.[27] The ability of this system to undergo photoinitiated electron collection on the rhodium center with the molecular architecture remaining intact is unprecedented and allows use in multielectron photochemistry.

Herein, we explore the design considerations for mixed-metal supramolecular complexes capable of photoinitiated electron collection providing insight into general molecular architectures for photocatalysts for solar energy driven hydrogen generation from water. Polymetallic complexes that couple ruthenium or osmium polyazine LAs to rhodium or iridium metal centers through BLs have been reported by Brewer[17,26,28−31] with many of interest as light-activated DNA photocleavage agents.[29−32] The redox, spectroscopic, and photophysical properties of these supramolecular complexes can be modulated by varying the metal, terminal ligands (TLs), and BLs, as shown in Figure 1.

The complexes $[\{(bpy)_2Ru(dpp)\}_2RhCl_2](PF_6)_5$,[26] $[\{(bpy)_2Os(dpp)\}_2RhCl_2](PF_6)_5$,[29] $[\{(tpy)RuCl(dpp)\}_2RhCl_2](PF_6)_3$,[30]

(20) (a) Heyduk, A. F.; Nocera, D. G. *Science* **2001**, *293*, 1639. (b) Rosenthal, J.; Bachman, J.; Dempsey, J. L.; Esswein, A. J.; Gray, T. G.; Hodgkiss, J. M.; Manke, D. R.; Luckett, T. D.; Pistorio, B. J.; Veige, A. S.; Nocera, D. G. *Coord. Chem. Rev.* **2005**, *249*, 1316. (c) Dempsey, J. L.; Esswein, A. J.; Manke, D. R.; Rosenthal, J.; Soper, J. D.; Nocera, D. G. *Inorg. Chem.* **2005**, *44*, 6879. (d) Esswein, A. J.; Veige, A. S.; Nocera, D. G. *J. Am. Chem. Soc.* **2005**, *127*, 16641.
(21) (a) Esswein, A. J.; Dempsey, J. L.; Nocera, D. G. *Inorg. Chem.* **2007**, *46*, 2362. (b) Cook, T. R.; Esswein, A. J.; Nocera, D. G. *J. Am. Chem. Soc.* **2007**, *129*, 10094.
(22) (a) Ozawa, H.; Haga, M.; Sakai, K. *J. Am. Chem. Soc.* **2006**, *128*, 4926. (b) Ozawa, H.; Yokoyama, Y.; Haga, M.; Sakai, K. *Dalton Trans.* **2007**, 1197.
(23) Rau, S.; Schäfer, B.; Gleich, D.; Anders, E.; Rudolph, M.; Friedrich, M.; Görls, H.; Henry, W.; Vos, J. G. *Angew. Chem., Int. Ed.* **2006**, *45*, 6215.
(24) Du, P.; Schneider, J.; Li, F.; Zhao, W.; Patel, U.; Castellano, F. N.; Eisenberg, R. *J. Am. Chem. Soc.* **2008**, *130*, 5056.
(25) Lei, P.; Hedlund, M.; Lomoth, R.; Rensmo, H.; Johansson, O.; Hammarström, L. *J. Am. Chem. Soc.* **2008**, *130*, 26.
(26) Elvington, M.; Brewer, K. J. *Inorg. Chem.* **2006**, *45*, 5242.
(27) Elvington, M.; Brown, J.; Arachchige, S. M.; Brewer, K. J. *J. Am. Chem. Soc.* **2007**, *129*, 10644.
(28) Arachchige, S. M.; Brown, J.; Brewer, K. J. *J. Photochem. Photobiol. A: Chem.* **2008**, *197*, 13.
(29) Holder, A. A.; Swavey, S.; Brewer, K. J. *Inorg. Chem.* **2004**, *43*, 303.
(30) Swavey, S.; Brewer, K. J. *Inorg. Chem.* **2002**, *41*, 4044.
(31) Zigler, D. F.; Mongelli, M. T.; Jeletic, M.; Brewer, K. J. *Inorg. Chem. Commun.* **2007**, *10*, 295.
(32) Holder, A. A.; Zigler, D. F.; Tarrago-Trani, M. T.; Storrie, B.; Brewer, K. J. *Inorg. Chem.* **2007**, *46*, 4760.

$[\{(tpy)OsCl(dpp)\}_2RhCl_2](PF_6)_3$,[31] and $[\{(bpy)_2Ru(dpb)\}_2IrCl_2](PF_6)_5$[17,33] have been previously reported with only $[\{(bpy)_2Ru(dpp)\}_2RhCl_2](PF_6)_5$ and $[\{(bpy)_2Ru(dpb)\}_2IrCl_2](PF_6)_5$ being shown to photochemically collect reducing equivalents, as shown in Figure 2. Preliminary studies of the photocatalysis of visible light-induced hydrogen production from water by $[\{(bpy)_2Ru(dpp)\}_2RhCl_2](PF_6)_5$[27] and $[\{(bpy)_2Ru(dpp)\}_2RhBr_2](PF_6)_5$[28] have been reported.

Experimental Section

Materials. The complexes $[\{(bpy)_2Ru(dpp)\}_2RhCl_2](PF_6)_5$,[27] $[\{(bpy)_2Ru(dpp)\}_2RhBr_2](PF_6)_5$,[28] $[\{(bpy)_2Os(dpp)\}_2RhCl_2](PF_6)_5$,[29] $[\{(tpy)RuCl(dpp)\}_2RhCl_2](PF_6)_3$,[30] $[\{(tpy)OsCl(dpp)\}_2RhCl_2](PF_6)_3$,[31] $[\{(bpy)_2Ru(dpb)\}_2IrCl_2](PF_6)_5$,[33] and $[(phen)_2Ru(dpp)](PF_6)_2$[34] were prepared as previously described. To ensure high purity needed for photophysical studies, the TL−LA−BL synthons were chromatographed on adsorption alumina three times, and the trimetallic complexes were recrystallyzed from hot ethanol to remove trace TL−LA−BL impurities. All materials were reagent grade and obtained from VWR Scientific or Aldrich Chemical Co. and used as received unless otherwise specified.

Synthesis of $[\{(phen)_2Ru(dpp)\}_2RhCl_2](PF_6)_5$. The complex $[\{(phen)_2Ru(dpp)\}_2RhCl_2](PF_6)_5$ was synthesized by heating at reflux for ca. 1 h $[(phen)_2Ru(dpp)](PF_6)_2$ (0.30 g, 0.30 mmol) and $RhCl_3 \cdot 3H_2O$ (0.045 g, 0.22 mmol) in a 2:1 $EtOH/H_2O$ (15 mL) mixture. The cooled solution was added dropwise to a saturated aqueous solution of KPF_6 (ca. 100 mL) to induce precipitation. The dark-red solid was washed with water (ca. 15 mL) and diethyl ether (ca. 100 mL), dried in a vacuum desiccator, dissolved in minimum volume of acetonitrile (ca. 10 mL), flash precipitated in diethyl ether (ca. 200 mL), followed by vacuum filtration to afford $[\{(phen)_2Ru(dpp)\}_2RhCl_2](PF_6)_5$ as a deep-red solid (0.20 g, 0.087 mmol, 58%). The high purity of the product needed for emission spectroscopy was achieved by careful purification of the $[(phen)_2Ru(dpp)](PF_6)_2$ starting material by adsorption chromatography on alumina. Electronic absorption spectroscopy in CH_3CN, λ_{max} ($\epsilon \times 10^{-4}$ $M^{-1}cm^{-1}$): 224 (11.5), 264 (11.6), 350 (3.76, sh), 418 (1.96), 520 (2.58). ESI-MS: $[M\text{-}PF_6]^+$, $m/z = 2145$.

Methods

Electronic Absorption Spectroscopy. Electronic absorption spectra were collected using a Hewlett-Packard 8452A diode array spectrophotometer (2 nm resolution) in spectroscopic grade acetonitrile (Burdick and Jackson). Measurements were repeated three times for extinction coefficients.

Electrochemistry. The cyclic voltammetry experiments were conducted with a Bioanalytical Systems (BAS) electrochemical analyzer. Potentials were referenced to a Ag/AgCl reference electrode (0.209 V vs NHE), which was calibrated against the $FeCp_2/FeCp_2^+$ redox couple[35] in 0.1 M Bu_4NPF_6 CH_3CN.

Emission Spectroscopy. The emission spectra were recorded in deoxygenated CH_3CN using a modified QuantaMaster Model QM-200−45E fluorimeter from Photon Technology Inc. modified to use a water cooled 150 W xenon arc lamp excitation source and thermoelectrically cooled Hamamatsu 1527 photomultiplier tube operating in photon counting mode with 0.25 nm resolution. The emission quantum yield, Φ^{em}, of $[\{(phen)_2Ru(dpp)\}_2RhCl_2](PF_6)_5$ was measured in deoxygenated CH_3CN by absorbance matching at the wavelength of excitation (520 nm) to the $[(bpy)_2Ru(dpp)Ru(bpy)_2](PF_6)_4$ standard with $\Phi^{em} = 0.00138$.[26]

Emission Lifetime Measurements. Excited state lifetime measurements were obtained using a Photon Technology Inc. PL-2300 nitrogen laser equipped with a PL-201 continuously tunable dye laser (360−900 nm) excitation source using a Hamamatsu R928 photomultiplier tube operating in direct analog mode. The signal was recorded on a LeCroy 9361 oscilloscope. The solutions were prepared in deoxygenated CH_3CN and excited at 520 nm. All decay curves were single exponential and fit to a linear function of the form $\ln[I_t - I_\infty] = \ln[I_0 - I_\infty] - [t/\tau]$, where I_t = signal at time t, I_∞ = signal at long times, I_0 = initial signal, t = time, and τ = lifetime of the excited state.

Photochemistry. The complexes were screened as photocatalysts for hydrogen production using the previously reported conditions for the $[\{(bpy)_2Ru(dpp)\}_2RhCl_2](PF_6)_5$ and DMA system.[27] The photolyses solutions consisted of the supramolecular complexes absorbance matched at the wavelength of excitation (470 nm) to have concentrations ranging from 50−118 μM, water (0.62 M, acidified to pH 2 with triflic acid), electron donor (1.5 M), and acetonitrile (final volume = 4.46 mL). The electron donors under investigation were DMA, TEA, and TEOA. The large excess of electron donor dictates solution pH. The effective pH values of the individual solutions were ~9.1, 14.7, and 11.8 for DMA, TEA, or TEOA electron donors, respectively, assuming that their pK_a values are not greatly perturbed relative to aqueous conditions ($pK_a = 5.07$ ($DMAH^+$), 10.75 ($TEAH^+$), and 7.76 ($TEOAH^+$)).[36] All solutions were deoxygenated before photolysis. Hydrogen quantification entailed headspace analysis using gas chromatography using a 580 GOW-MAC gas chromatograph equipped with a 5 Å molecular sieves column using ultrahigh purity argon as the carrier gas, equipped with a rhenium tungsten thermal conductivity detector. The total amount of hydrogen produced in a photolysis experiment was obtained by the sum of the hydrogen in the headspace and in solution. The amount of hydrogen in the solution was calculated according to Henry's Law using the saturation mole fraction of hydrogen in acetonitrile as 1.78×10^{-4}.[37] Dissolved hydrogen accounts for ca. 21% of the total hydrogen produced. Stirring of a photolysis solution for two hours at room temperature did not result in changes in the amount of H_2 detected in the headspace. The reported micromoles of hydrogen are the

(33) (a) Bridgewater, J. S.; Vogler, L. M.; Molnar, S. M.; Brewer, K. J. *Inorg. Chim. Acta* **1993**, *208*, 179. (b) Molnar, S. M.; Jensen, G. E.; Vogler, L. M.; Jones, S. W.; Laverman, L.; Bridgewater, J. S.; Richter, M. M.; Brewer, K. J. *J. Photochem. Photobiol. A: Chem.* **1994**, *80*, 315.
(34) Wallace, A. W., Jr.; Petersen, J. D. *Inorg. Chim. Acta* **1989**, *166*, 47.
(35) Gennett, T.; Milner, D. F.; Weaver, M. J. *J. Phys. Chem.* **1985**, *89*, 2787.
(36) *CRC Handbook of Chemistry and Physics, 88th Edition (Internet Version 2008)*; Lide, D. R., Ed.; CRC Press/Taylor and Francis: Boca Raton, FL.
(37) Purwanto; Deshpande, R. M.; Chaudhari, R. V.; Delmas, H. *J. Chem. Eng. Data* **1996**, *41*, 1414.

average of three trials. Photolyses were conducted using a light emitting diode (LED) array constructed locally with flat optical bottom cells.[38] The LEDs were all set to the same power output prior to the experiment using a Scientech, Inc. (Boulder, CO) Mentor MA10 power meter with a MC 2501 calorimeter head unit. Validation of the LED array was achieved using the potassium tris(oxalato)ferrate(II) actinometer.[39] The effect of the wavelength of excitation on hydrogen production was analyzed by irradiating the solutions at 470 nm (light flux = 9.3×10^{18} photons/min) and 520 nm (light flux = 4.7×10^{19} photons/min) using 5 W blue and green LEDs, respectively.

Results and Discussion

Supramolecular complexes composed of two Ru(II) or Os(II) polyazine LAs with TLs, coupled through polyazine BLs to a central Ir(III) or Rh(III) have been prepared and assayed as photocatalysts for hydrogen production via photoinitiated electron collection. The complexes have spectroscopic, redox, and photochemical properties dictated by the components. The supramolecular assemblies provide TL−LA−BL−M′X_2−BL−LA−TL molecular architectures (M′ = Rh(III) or Ir(III) and X = Cl or Br). The TLs used are two bpy, two phen, or tpy and Cl ligands. The BLs are typically dpp, whereas the Ir(III) system uses the dpb ligand. The complexes possess intense MLCT transitions in the visible region of the spectrum, making them efficient LAs. Light absorption is dictated by the TL−LA−BL subunit. A series of mixed-metal trimetallic complexes containing this structural motif have been designed that probe the impact of subunit variation on photocatalytic hydrogen production from water.

Synthesis. The synthesis of the mixed-metal trimetallic complexes uses a building-block approach with the incorporation of the reactive Rh(III) metal center being the final step.[28−31] The new complex [{(phen)$_2$Ru(dpp)}$_2$RhCl$_2$](PF$_6$)$_5$ was prepared using a similar synthetic approach as [{(bpy)$_2$Ru(dpp)}$_2$RhCl$_2$](PF$_6$)$_5$[27,28] with [(phen)$_2$Ru(dpp)](PF$_6$)$_2$, and $RhCl_3 \cdot 3H_2O$ heated at reflux in ∼2:1 stoichiometry in a EtOH/H_2O mixture for ∼1 h. ESI mass spectrometry analysis of the complex was consistent with its formulation.

Electrochemistry. The electrochemical data of the new complex [{(phen)$_2$Ru(dpp)}$_2$RhCl$_2$](PF$_6$)$_5$ and the previously reported complexes [{(bpy)$_2$Ru(dpp)}$_2$RhCl$_2$](PF$_6$)$_5$, [{(bpy)$_2$Ru(dpp)}$_2$RhBr$_2$](PF$_6$)$_5$, [{(bpy)$_2$Ru(dpb)}$_2$IrCl$_2$](PF$_6$)$_5$, [{(tpy)RuCl(dpp)}$_2$RhCl$_2$](PF$_6$)$_3$, [{(tpy)OsCl(dpp)}$_2$RhCl$_2$](PF$_6$)$_3$, and [{(bpy)$_2$Os(dpp)}$_2$RhCl$_2$](PF$_6$)$_5$ are summarized in Table 1 and require examination to understand photocatalyst functioning.

The cyclic voltammogram of [{(phen)$_2$Ru(dpp)}$_2$RhCl$_2$](PF$_6$)$_5$ is shown in Figure 3 with the others provided in the Supporting Information. All of the trimetallics show overlapping $Ru^{II/III}$- or $Os^{II/III}$-based oxidations, indicating the absence of significant intercomponent coupling between the ruthenium or osmium subunits.[17,26−31,33] The ΔE_p ($\Delta E_p = E_p^a - E_p^c$) for these $Ru^{II/III}$ or $Os^{II/III}$ couples are ca. 120 mV, indicating two closely spaced one-electron couples. The $Os^{II/III}$-based oxidations in [{(tpy)OsCl(dpp)}$_2$RhCl$_2$](PF$_6$)$_3$[31] and [{(bpy)$_2$Os(dpp)}$_2$RhCl$_2$](PF$_6$)$_5$[29] occur at less-positive potentials relative to the analogous ruthenium-based systems,[30,26,27] consistent with the higher-energy dπ orbitals on osmium. The $Ru^{II/III}$ oxidation in [{(bpy)$_2$Ru(dpp)}$_2$RhCl$_2$](PF$_6$)$_5$, [{(bpy)$_2$Ru(dpp)}$_2$RhBr$_2$](PF$_6$)$_5$, and [{(phen)$_2$Ru(dpp)}$_2$RhCl$_2$](PF$_6$)$_5$ occurs at ∼1.81 V versus NHE, whereas the $Ru^{II/III}$ oxidation for the [{(tpy)RuCl(dpp)}$_2$RhCl$_2$](PF$_6$)$_3$ occurs at a less positive potential of 1.33 V versus NHE attributed to the tpy and chloride coordination to ruthenium in lieu of two bpy ligands making the ruthenium center more electron rich. A similar shift is observed in the $Os^{II/III}$

Table 1. Electrochemical Properties of a Series of Mixed-Metal Trimetallic Complexes (bpy = 2,2′-Bipyridine, tpy = 2,2′:6′,2″-Terpyridine, phen = 1,10-Phenanthroline, dpp = 2,3-Bis(2-pyridyl)pyrazine, dpb = 2,3-Bis(2-pyridyl)benzoquinoxaline).

complex	$E_{1/2}$ in V[a]	assignment
[{(bpy)$_2$Ru(dpp)}$_2$RhCl$_2$](PF$_6$)$_5$[b]	1.84	$2Ru^{II/III}$
	−0.16[c]	$Rh^{III/II/I}$
	−0.55	dpp,dpp/dpp,dpp$^-$
	−0.79	dpp,dpp$^-$/dpp$^-$,dpp$^-$
[{(bpy)$_2$Ru(dpb)}$_2$IrCl$_2$](PF$_6$)$_5$[d]	1.77	$2Ru^{II/III}$
	0.24	dpb,dpb/dpb,dpb$^-$
	0.08	dpb,dpb$^-$/dpb$^-$,dpb$^-$
[{(tpy)RuCl(dpp)}$_2$RhCl$_2$](PF$_6$)$_3$[e]	1.33	$2Ru^{II/III}$
	−0.26[c]	$Rh^{III/II/I}$
	−0.66	dpp,dpp/dpp,dpp$^-$
	−0.99	dpp,dpp$^-$/dpp$^-$,dpp$^-$
[{(tpy)OsCl(dpp)}$_2$RhCl$_2$](PF$_6$)$_3$[f]	1.05	$2Os^{II/III}$
	−0.30[c]	$Rh^{III/II/I}$
	−0.65	dpp,dpp/dpp,dpp$^-$
	−0.99	dpp,dpp$^-$/dpp$^-$,dpp$^-$
[{(bpy)$_2$Os(dpp)}$_2$RhCl$_2$](PF$_6$)$_5$[g]	1.42	$2Os^{II/III}$
	−0.18[c]	$Rh^{III/II/I}$
	−0.55	dpp,dpp/dpp,dpp$^-$
	−0.79	dpp,dpp$^-$/dpp$^-$,dpp$^-$
[{(bpy)$_2$Ru(dpp)}$_2$RhBr$_2$](PF$_6$)$_5$[h]	1.80	$2Ru^{II/III}$
	−0.12[c]	$Rh^{III/II/I}$
	−0.51	dpp,dpp/dpp,dpp$^-$
	−0.81	dpp,dpp$^-$/dpp$^-$,dpp$^-$
[{(phen)$_2$Ru(dpp)}$_2$RhCl$_2$](PF$_6$)$_5$	1.78	$2Ru^{II/III}$
	−0.18[c]	$Rh^{III/II/I}$
	−0.59	dpp,dpp/dpp,dpp$^-$
	−0.85	dpp,dpp$^-$/dpp$^-$,dpp$^-$

[a] Potentials reported versus the NHE reference electrode in 0.1 M Bu_4NPF_6 in CH_3CN. [b] Refs 26 and 27. [c] Irreversible E_p^c reported. [d] Ref 33. [e] Ref 30. [f] Ref 31. [g] Ref 29. [h] Ref 28.

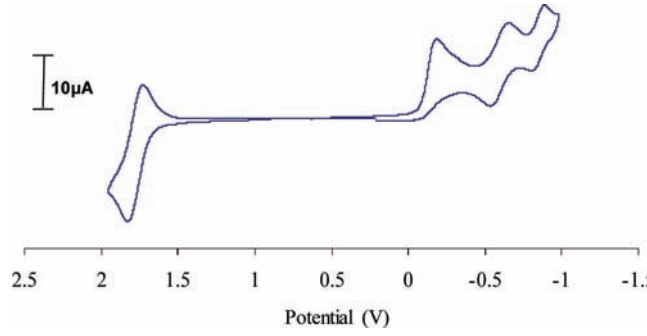

Figure 3. Cyclic voltammogram of [{(phen)$_2$Ru(dpp)}$_2$RhCl$_2$]((PF$_6$)$_5$ measured in 0.1 M Bu_4NPF_6/CH_3CN at RT (bpy = 2,2′-bipyridine, phen = 1,10-phenanthroline, dpp = 2,3-bis(2-pyridyl)pyrazine). Potentials reported in volts vs NHE.

(38) Brown, J. R.; Elvington, M.; Mongelli, M. T.; Zigler, D. F.; Brewer, K. J. *Proc. SPIE-Opt. Photo. Sol. Hydrogen Nanotechnol.* **2006**, *6340*, 634007W1.

(39) Rabek, J. F. *Experimental Methods in Photochemistry and Photophysics*; John Wiley and Sons Ltd.: New York, 1982.

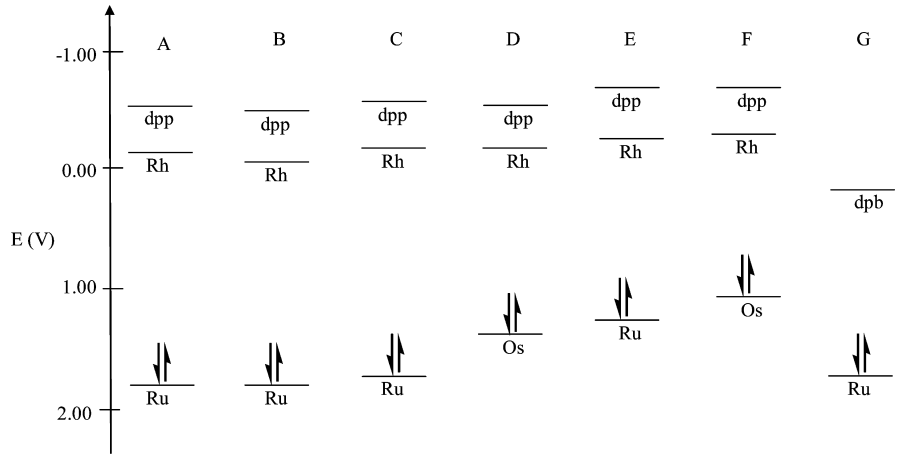

Figure 4. Frontier orbital energetics for mixed-metal trimetallic complexes simplified by showing single orbitals from orbital sets with *E* in volts vs NHE obtained from cyclic voltammetry (A = $[\{(bpy)_2Ru(dpp)\}_2RhCl_2](PF_6)_5$, B = $[\{(bpy)_2Ru(dpp)\}_2RhBr_2](PF_6)_5$, C = $[\{(phen)_2Ru(dpp)\}_2RhCl_2](PF_6)_5$, D = $[\{(bpy)_2Os(dpp)\}_2RhCl_2](PF_6)_5$, E = $[\{(tpy)RuCl(dpp)\}_2RhCl_2](PF_6)_3$, F = $[\{(tpy)OsCl(dpp)\}_2RhCl_2](PF_6)_3$, and G = $[\{(bpy)_2Ru(dpb)\}_2IrCl_2](PF_6)_5$). (bpy = 2,2′-bipyridine, phen = 1,10-phenanthroline, dpp = 2,3-bis(2-pyridyl)pyrazine, tpy = 2,2′:6′,2″-terpyridine, dpb = 2,3-bis(2-pyridyl)benzoquinoxaline).

oxidation potential of $[\{(tpy)OsCl(dpp)\}_2RhCl_2](PF_6)_3$. The electrochemical properties illustrate the terminal metal-based nature of the highest occupied molecular orbital (HOMO) with energy tuned by metal and TL variation. The reductive electrochemistry of the rhodium-based systems display irreversible $Rh^{III/II/I}$ reductions, followed by two sequential reversible reductions of each BL, dpp,dpp/dpp,dpp$^-$, and dpp,dpp$^-$/dpp$^-$,dpp$^-$. The $Rh^{III/II/I}$ reduction is followed by the loss of halides, similar to that reported for $[Rh(bpy)_2Cl_2]^+$.[40] The reductive electrochemistry of these rhodium centered complexes shows the close energetic proximity of the Rh(dσ*) and dpp(π*) orbitals in this molecular architecture. The electrochemical properties of $[\{(phen)_2Ru(dpp)\}_2RhCl_2](PF_6)_5$ are quite similar to those of $[\{(bpy)_2Ru(dpp)\}_2RhCl_2](PF_6)_5$ and $[\{(bpy)_2Ru(dpp)\}_2RhBr_2](PF_6)_5$. The $Rh^{III/II/I}$ reduction in $[\{(bpy)_2Ru(dpp)\}_2RhBr_2](PF_6)_5$ occurs at −0.12 V versus NHE, 40 mV more positive than the chloride analogue $[\{(bpy)_2Ru(dpp)\}_2RhCl_2](PF_6)_5$, consistent with the weaker σ-donor ability of Br^- versus Cl^-. The $Rh^{III/II/I}$ reductions for $[\{(tpy)RuCl(dpp)\}_2RhCl_2](PF_6)_3$ and $[\{(tpy)OsCl(dpp)\}_2RhCl_2](PF_6)_3$ are shifted to more negative potentials of −0.26 and −0.30 V versus NHE consistent with more electron-rich LA metals in these complexes and lower cationic charge. All of the rhodium centered complexes used in this study were selected to have rhodium localized LUMOs.

The iridium-based complex $[\{(bpy)_2Ru(dpb)\}_2IrCl_2](PF_6)_5$ possesses dpb BLs with much lower lying π*-acceptor orbitals and an iridium center with higher-energy dσ* orbitals. The reductive electrochemistry of $[\{(bpy)_2Ru(dpb)\}_2IrCl_2](PF_6)_5$ displays four sequential dpb reductions, with each dpb being reduced by one and then two electrons with no iridium reduction observed in the CH_3CN/Bu_4NPF_6 electrochemical window.[33] The electrochemistry of the rhodium-based trimetallics predicts the Ru(dπ) nature of the HOMOs and the Rh(dσ*) nature of the LUMOs, allowing the rhodium to function as an electron collector and a lowest-lying Ru(dπ) → Rh(dσ*) metal-to-metal charge-transfer (^{3}MMCT) excited state.[26−30] By contrast, the electrochemistry of $[\{(bpy)_2Ru(dpb)\}_2IrCl_2](PF_6)_5$ predicts a Ru(dπ)-based HOMO and a dpb(π*)-based LUMO in which the Ir(dσ*) orbitals are energetically inaccessible.[17,33] The variation of the frontier orbital energetics for the mixed-metal complexes are illustrated in Figure 4. The tuning of the orbital energetics provided by TL, LA, BL, and the central metal will allow for study of the impact of orbital energies and identity on observed photochemistry. All complexes are predicted to have low-energy M(dπ)→BL(π*) CT transitions that vary according to the illustrated electrochemical energy gap (M = Ru or Os).

Electronic Absorption Spectroscopy. The electronic absorption spectra of complexes are shown in Figure 5. The lowest-lying absorptions, λ_{max}^{abs}, are provided in Table 2. Individual spectra are in the Supporting Information.

(40) Kew, G.; DeArmond, K.; Hanck, K. *J. Phys. Chem.* **1974**, *78*, 727.
(41) (a) Rasmussen, S. C.; Richter, M. M.; Yi, E.; Place, H.; Brewer, K. J. *Inorg. Chem.* **1990**, *29*, 3926. (b) Kalyanasundaram, K.; Graetzel, M.; Nazeeruddin, M. K. *J. Phys. Chem.* **1992**, *96*, 5865.
(42) Caspar, J. V.; Kober, E. M.; Sullivan, B. P.; Meyer, T. J. *J. Am. Chem. Soc.* **1982**, *104*, 630.

(43) [i]The λ_{max}^{em} $[\{(tpy)RuCl(dpp)\}_2RhCl_2](PF_6)_3$ was predicted using the difference in energy between the λ_{max}^{abs} from the Ru(dπ) → dpp(π*) ^{1}MLCT and λ_{max}^{em} from the Ru(dπ) → dpp(π*) ^{3}MLCT of the model complex $[(tpy)RuCl(dpp)](PF_6)$[44] and adjusting the λ_{max}^{abs} for $[\{(tpy)RuCl(dpp)\}_2RhCl_2](PF_6)_3$ by this factor. [j]Used the difference in energy between the λ_{max}^{em} from the Ru(dπ) → dpp(π*) ^{3}MLCT and λ_{max}^{em} from the Os(dπ) → dpp(π*) ^{3}MLCT of the model complexes $[(bpy)_2M(dpp)](PF_6)_2$ (M = Ru or Os, respectively)[45] and adjusted the λ_{max}^{em} for $[(tpy)RuCl(dpp)](PF_6)$ to predict the λ_{max}^{em} from the Os(dπ) → dpp(π*) ^{3}MLCT of the model complex $[(tpy)OsCl(dpp)](PF_6)$. The λ_{max}^{em} for $[\{(tpy)OsCl(dpp)\}_2RhCl_2](PF_6)_3$ was predicted using the difference in energy between the λ_{max}^{abs} from the Os(dπ) → dpp(π*) ^{1}MLCT and the predicted λ_{max}^{em} from the Os(dπ) → dpp(π*) ^{3}MLCT of the model complex $[(tpy)OsCl(dpp)](PF_6)$ and adjusting the λ_{max}^{abs} absorption for $[\{(tpy)OsCl(dpp)\}_2RhCl_2](PF_6)_3$ by this factor. [k,l] The λ_{max}^{em} for $[\{(bpy)_2M(BL)\}_2M'Cl_2](PF_6)_5$ (M = Os, BL = dpp, M′ = Rh or M = Ru, BL = dpb, M′ = Ir) was predicted using the difference in energy between the λ_{max}^{abs} from the M(dπ) → BL(π*) ^{1}MLCT and λ_{max}^{em} from the M(dπ) → BL(π*) ^{3}MLCT (M = Os, BL = dpp or M = Ru, BL = dpb) of the model complexes $[(bpy)_2M(BL)](PF_6)_2$ (M = Os, BL = dpp or M = Ru, BL = dpb)[45,46] and adjusting the λ_{max}^{abs} absorption for $[\{(bpy)_2M(BL)\}_2M'Cl_2](PF_6)_5$ (M = Os, BL = dpp, M′ = Rh or M = Ru, BL = dpb, M′ = Ir.
(44) Vogler, L. M.; Franco, C.; Jones, S. W.; Brewer, K. J. *Inorg. Chim. Acta* **1994**, *221*, 55.

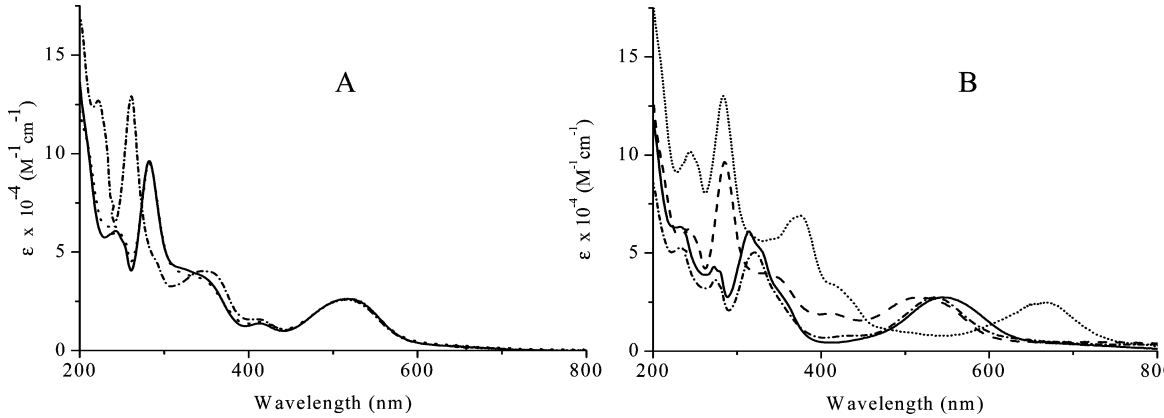

Figure 5. Electronic absorption spectra of $[\{(bpy)_2Ru(dpp)\}_2RhCl_2](PF_6)_5$ (—), $[\{(bpy)_2Ru(dpp)\}_2RhBr_2](PF_6)_5$ (– – –), and $[\{(phen)_2Ru(dpp)\}_2RhCl_2](PF_6)_5$ (-•-) (A); $[\{(bpy)_2Ru(dpb)\}_2IrCl_2](PF_6)_5$ (•••), $[\{(tpy)RuCl(dpp)\}_2RhCl_2](PF_6)_3$ (—), $[\{(tpy)OsCl(dpp)\}_2RhCl_2](PF_6)_3$ (-•-), and $[\{(bpy)_2Os(dpp)\}_2RhCl_2](PF_6)_5$ (---) (B); in acetonitrile at room temperature (bpy = 2,2′-bipyridine, phen = 1,10-phenanthroline, dpp = 2,3-bis(2-pyridyl)pyrazine, tpy = 2,2′:6′,2″-terpyridine, dpb = 2,3-bis(2-pyridyl)benzoquinoxaline).

Table 2. Spectroscopic and Photophysical Properties of Mixed-Metal Trimetallic Complexes (bpy = 2,2′-Bipyridine, tpy = 2,2′:6′,2″-Terpyridine, phen = 1,10-Phenanthroline, dpp = 2,3-Bis(2-pyridyl)pyrazine, dpb = 2,3-Bis(2-pyridyl)benzoquinoxaline)

complex	λ_{max}^{abs} (nm) ^{1}MLCT[a]	λ_{max}^{em} (nm) ^{3}MLCT[a]	τ (ns)[a]	$E(*CAT^{n+}/CAT^{(n-1)+})$ ^{3}MLCT (V)[b]	$E(*CAT^{n+}/CAT^{(n-1)+})$ ^{3}MMCT (V)[b]
$[\{(bpy)_2Ru(dpp)\}_2RhCl_2](PF_6)_5$	520[c]	760	23	1.47	1.08
$[\{(bpy)_2Ru(dpp)\}_2RhBr_2](PF_6)_5$	520[d]	760	26	1.51	1.12
$[\{(phen)_2Ru(dpp)\}_2RhCl_2](PF_6)_5$	520	746	27	1.49	1.08
$[\{(tpy)RuCl(dpp)\}_2RhCl_2](PF_6)_3$	540[e]	(820)[i]		1.25	0.85
$[\{(tpy)OsCl(dpp)\}_2RhCl_2](PF_6)_3$	538[f]	(980)[i]		0.95	0.61
$[\{(bpy)_2Os(dpp)\}_2RhCl_2](PF_6)_5$	530[g]	(930)[i]		1.15	0.78
$[\{(bpy)_2Ru(dpb)\}_2IrCl_2](PF_6)_5$	666[h]	(1100)[i]	–	1.37	–

[a] Spectra obtained in deoxygenated acetonitrile at room temperature. [b] V vs NHE, $E(*CAT^{n+}/CAT^{(n-1)+})$ = excited state reduction potential. [c] Ref 26. [d] Ref 28. [e] Ref 30. [f] Ref 31. [g] Ref 29. [h] Ref 33. [i] No emission is observed, λ_{max}^{em} estimated based on shifts in absorption vs emission from monometallic synthons and absorption energy of the trimetallic complex.[43−46]

The trimetallic complexes are efficient LAs with transitions characteristic of each subunit in the TL−LA−BL assembly. The TL−LA−BL assembly-based electronic absorption spectra is evidenced by the near spectroscopic identity of $[\{(bpy)_2Ru(dpp)\}_2RhCl_2](PF_6)_5$ and $[\{(bpy)_2Ru(dpp)\}_2RhBr_2](PF_6)_5$.[26,28] The UV region of the spectrum of all of the complexes is dominated by TL (bpy, tpy, or phen) and BL (dpp or dpb) based $\pi \rightarrow \pi^*$ transitions with the BL based transitions occurring at lower energies. The visible region is dominated by $M(d\pi) \rightarrow TL(\pi^*)$ or $M(d\pi) \rightarrow BL(\pi^*)$ MLCT transitions with the lowest-energy transition being $M(d\pi) \rightarrow BL(\pi^*)$ CT in nature (M = Ru or Os, BL = dpp or dpb). The $Ru(d\pi) \rightarrow bpy(\pi^*)$ CT and $Ru(d\pi) \rightarrow dpp(\pi^*)$ CT transitions for $[\{(bpy)_2Ru(dpp)\}_2RhX_2](PF_6)_5$ occur in the visible region with the lowest-energy transition being $Ru(d\pi) \rightarrow dpp(\pi^*)$ CT in nature occurring at 520 nm, $\epsilon = 2.6 \times 10^4\ M^{-1}cm^{-1}$. The similarity between the two spectra suggests that the light absorption properties of these two molecules are not greatly perturbed by substitution of the chloride with bromide on the rhodium center. The visible region of the electronic absorption spectrum of $[\{(phen)_2Ru(dpp)\}_2RhCl_2](PF_6)_5$ is also very similar with the lowest-energy transition being $Ru(d\pi) \rightarrow dpp(\pi^*)$ CT in nature ($\lambda_{max}^{abs} = 520$ nm, $\epsilon = 2.6 \times 10^4\ M^{-1}cm^{-1}$). The electronic absorption spectra of the ruthenium and osmium analogues of $[\{(bpy)_2M(dpp)\}_2RhCl_2](PF_6)_5$ or $[\{(tpy)MCl(dpp)\}_2RhCl_2](PF_6)_3$ (M = Ru or Os) are very similar with the $Os(d\pi) \rightarrow dpp(\pi^*)$ CT transitions occurring at slightly lower energy. The osmium analogues possess significant intensity in the lower-energy tail of the $Os(d\pi) \rightarrow dpp(\pi^*)$ CT transitions, representing direct population of the ^{3}MLCT state, gaining intensity by the significant spin−orbit coupling in osmium. The $M(d\pi) \rightarrow dpp(\pi^*)$ CT transition at ~540 nm for the $[\{(tpy)MCl(dpp)\}_2RhCl_2](PF_6)_3$ (M = Ru or Os)[30,31] complexes are red-shifted relative to those of $[\{(bpy)_2M(dpp)\}_2RhCl_2](PF_6)_5$ (M = Ru or Os), consistent with the higher-energy $M(d\pi)$ (M = Ru or Os) orbitals in $[\{(tpy)MCl(dpp)\}_2RhCl_2](PF_6)_3$. The red-shifted MLCT transitions agree well with the electrochemical properties of $[\{(tpy)MCl(dpp)\}_2RhCl_2](PF_6)_3$ (M = Ru or Os), which shows a more electron-rich, easier to oxidize metal center. The $Ru(d\pi) \rightarrow dpb(\pi^*)$ MLCT transition in $[\{(bpy)_2Ru(dpb)\}_2IrCl_2](PF_6)_5$ is considerably red-shifted relative to the dpp analogues, consistent with the lower energy of the $dpb(\pi^*)$ orbitals of $[\{(bpy)_2Ru(dpb)\}_2IrCl_2](PF_6)_5$.[33]

The spectroscopy and the electrochemistry of these trimetallic complexes provide insight into the expected photophysical and photochemical properties. Incorporation of a Rh(III) center into the molecular assemblies affords low-lying MMCT states resulting from low-lying $Rh(d\sigma^*)$ orbitals, below the dpp BL π^*-acceptor orbitals, as seen in Figure 6. The electronic absorption spectroscopy predicts a low-lying, optically populated $Ru(d\pi) \rightarrow dpp(\pi^*)$ CT state

(45) Abdel-Shafi, A. A.; Worrall, D. R.; Ershov, A. Y. *Dalton Trans.* **2004**, 30.
(46) Molnar, S. M.; Neville, K. R.; Jensen, G. E.; Brewer, K. J. *Inorg. Chim. Acta* **1993**, *206*, 69.

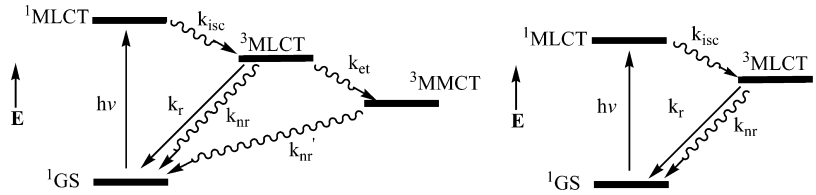

Figure 6. Energy-state diagram for rhodium-centered supramolecular assemblies incorporating low-lying MMCT states showing only lowest-lying excited states (left) and for the iridium centered supramolecular assembly incorporating low-lying MLCT states (right). GS = ground state, MLCT = metal-to-ligand charge-transfer, MMCT = metal-to-metal charge transfer, k_r = rate constant for radiative decay, k_{nr} = rate constant for nonradiative decay, k_{isc} = rate constant for intersystem crossing, k_{et} = rate constant for electron transfer.

in these supramolecular complexes. The Ru(dπ) → dpp(π^*) CT states, once optically populated, are known to undergo intersystem crossing to populate the often emissive ^{3}MLCT state. In the rhodium centered complexes, the Rh(dσ^*) LUMO provides for facile intramolecular electron transfer to produce the Ru(dπ) → Rh(dσ^*) ^{3}MMCT state. Electrochemistry shows the ability of the Rh(III) to be reduced by two electrons to Rh(I), predicting that these rhodium centered systems should be able to photochemically collect electrons at the rhodium center. This property of the rhodium-centered systems can be exploited to promote multielectron catalysis such as the reduction of water to hydrogen.

Emission Spectroscopy and Photophysics. Ruthenium polyazine complexes display optically populated ^{1}MLCT states that typically intersystem cross with unit efficiency to the ^{3}MLCT states that are often emissive, providing a probe into excited-state dynamics. Similar to [{(bpy)$_2$Ru(dpp)}$_2$-RhCl$_2$](PF$_6$)$_5$,[26] the complexes [{(bpy)$_2$Ru(dpp)}$_2$RhBr$_2$]-(PF$_6$)$_5$[28] and [{(phen)$_2$Ru(dpp)}$_2$RhCl$_2$](PF$_6$)$_5$ have been found to display weak emissions from the Ru(dπ) → dpp(π^*) ^{3}MLCT state at λ^{em}_{max} = 760 nm (emission quantum yield, $\Phi^{em} = 1.5 \times 10^{-4}$) and λ^{em}_{max} = 746 nm ($\Phi^{em} = 1.8 \times 10^{-4}$) respectively, at room temperature in deoxygenated acetonitrile solutions following Ru(dπ) → dpp(π^*) ^{1}MLCT excitation at 520 nm. Compared to the model system [(bpy)$_2$Ru(dpp)Ru(bpy)$_2$](PF$_6$)$_4$, which lacks a rhodium electron acceptor, λ^{em}_{max} = 744 nm, $\Phi^{em} = 1.38 \times 10^{-3}$, the emission from the Ru(dπ) → dpp(π^*) ^{3}MLCT state of [{(bpy)$_2$Ru(dpp)}$_2$RhBr$_2$](PF$_6$)$_5$ and [{(phen)$_2$Ru(dpp)}$_2$-RhCl$_2$](PF$_6$)$_5$ are reduced by 89 and 87%, respectively, due to intramolecular electron transfer to produce the Ru(dπ)→Rh(dσ^*) ^{3}MMCT states, Figure 6. This compares well with the reported λ^{em}_{max} = 760 nm, $\Phi^{em} = 7.3 \times 10^{-5}$, and 95% quenching of the ^{3}MLCT emission observed in [{(bpy)$_2$Ru(dpp)}$_2$RhCl$_2$](PF$_6$)$_5$ hydrogen photocatalyst.[26] Energy transfer to the ligand field (^{3}LF) of rhodium would also provide for ^{3}MLCT emission quenching but is expected to be uphill.[41] The rates of electron transfer to populate the ^{3}MMCT from the ^{3}MLCT state for [{(bpy)$_2$Ru(dpp)}$_2$-RhBr$_2$](PF$_6$)$_5$[28] and [{(phen)$_2$Ru(dpp)}$_2$RhCl$_2$](PF$_6$)$_5$ are determined to be $k_{et} = 5.2 \times 10^7$ and 4.4×10^7 s^{-1} respectively, comparable to the $k_{et} = 1.2 \times 10^8$ s^{-1} reported for [{(bpy)$_2$Ru(dpp)}$_2$RhCl$_2$](PF$_6$)$_5$[26] (assuming that k_r and k_{nr} of these complexes are the same as the model system used). The excited-state lifetimes of the ^{3}MLCT states have been measured for [{(bpy)$_2$Ru(dpp)}$_2$RhCl$_2$](PF$_6$)$_5$, [{(bpy)$_2$Ru-(dpp)}$_2$RhBr$_2$](PF$_6$)$_5$, and [{(phen)$_2$Ru(dpp)}$_2$RhCl$_2$](PF$_6$)$_5$ in deoxygenated acetonitrile solution at room temperature and are very similar, 32, 26, and 27 ns, respectively. The other mixed-metal trimetallic complexes under investigation do not display detectable emissions in the visible region following excitation of M(dπ) → dpp(π^*) (M = Ru or Os) CT transition. This is not surprising considering the expected lower-energy ^{3}MLCT in these systems. Estimation of the energies of these ^{3}MLCT states are provided in Table 2. Generally, lower-energy ^{3}MLCT states display weaker, shorter-lived emissions consistent with the energy gap law.[42]

Photochemistry. The supramolecular architectures provide complexes that are efficient LAs throughout the UV and visible region of the electromagnetic spectrum that should be able to photochemically collect electrons when photolyzed in the presence of a suitable electron donor. We recently established the first supramolecular photoinitiated electron collector, [{(bpy)$_2$Ru(dpp)}$_2$RhCl$_2$](PF$_6$)$_5$, to photochemically produce hydrogen from water with a $\Phi \approx 0.01$.[27] This molecule functions by photolysis in the presence of an electron donor, facilitating electron collection to afford the Rh(I) complex, [{(bpy)$_2$Ru(dpp)}$_2$Rh^I]$^{5+}$, and two chlorides. In the presence of water and an electron donor, this system can reduce water to hydrogen. Similar to [{(bpy)$_2$Ru(dpp)}$_2$-RhCl$_2$](PF$_6$)$_5$, the complexes [{(bpy)$_2$Ru(dpp)}$_2$RhBr$_2$](PF$_6$)$_5$, [{(phen)$_2$Ru(dpp)}$_2$RhCl$_2$](PF$_6$)$_5$, [{(bpy)$_2$Os(dpp)}$_2$RhCl$_2$]-(PF$_6$)$_5$, [{(tpy)RuCl(dpp)}$_2$RhCl$_2$](PF$_6$)$_3$, and [{(tpy)OsCl-(dpp)}$_2$RhCl$_2$](PF$_6$)$_3$ all have charge transfer LAs as well as a central rhodium center, which acts as the site of localization of the LUMO. The photochemical and electrochemical properties of these molecules have been modulated by component modification and the impact of the orbital energetics on the photocatalysis of water reduction is explored. Through previous studies, we have established that [{(bpy)$_2$Ru(dpb)}$_2$IrCl$_2$](PF$_6$)$_5$ affords photoinitiated electron collection on dpb to generate the doubly reduced species [{(bpy)$_2$Ru(dpb$^-$)}$_2$IrCl$_2$]$^{3+}$.[17] In this complex, the BL acts as the site of localization of the LUMO and the collected electrons reside on the BLs bound to the iridium center. The role of the rhodium-based electron collector is understood by the comparison of this iridium-based system to the photocatalytic system.

Mixed-metal trimetallic complexes were assayed for photocatalytic efficiency using the conditions previously studied for [{(bpy)$_2$Ru(dpp)}$_2$RhCl$_2$](PF$_6$)$_5$.[27] The metal complex was dissolved in acetonitrile, and combined with water acidified to pH 2 with triflic acid and DMA. The photolyses were carried out under an argon atmosphere and

Table 3. Photocatalysis of Water Reduction to Produce Hydrogen Using Mixed-Metal Supramolecular Complexes (bpy = 2,2′-Bipyridine, tpy = 2,2′:6′,2″-Terpyridine, phen = 1,10-Phenanthroline, dpp = 2,3-Bis(2-pyridyl)pyrazine, dpb = 2,3-Bis(2-pyridyl)benzoquinoxaline)

complex	complex (μM)[a]	electron donor[b]	H_2O (M)[a]	H_2 (470 nm) (μmol)[c]	H_2 (520 nm) (μmol)[c]	E_{redox} ^{3}MLCT (V)[d]
$[\{(bpy)_2Ru(dpp)\}_2RhCl_2](PF_6)_5$	65	DMA	0.62	6.0 ± 0.7	1.9 ± 0.2	0.42
$[\{(bpy)_2Ru(dpp)\}_2RhBr_2](PF_6)_5$	65	DMA	0.62	7.2 ± 0.8	1.8 ± 0.5	0.46
$[\{(phen)_2Ru(dpp)\}_2RhCl_2](PF_6)_5$	65	DMA	0.62	5.4 ± 0.5	2.2 ± 0.2	0.44
$[\{(bpy)_2Ru(dpb)\}_2IrCl_2](PF_6)_5$	88	DMA	0.62	<0.02	<0.02	0.32
$[\{(bpy)_2Os(dpp)\}_2RhCl_2](PF_6)_5$	50	DMA	0.62	0.13 ± 0.03	<0.02	0.10
$[\{(tpy)RuCl(dpp)\}_2RhCl_2](PF_6)_3$	118	DMA	0.62	0.21 ± 0.06	<0.02	0.20
$[\{(tpy)OsCl(dpp)\}_2RhCl_2](PF_6)_3$	92	DMA	0.62	<0.02	<0.02	−0.10
$[\{(bpy)_2Ru(dpp)\}_2RhCl_2](PF_6)_5$	65	TEA	0.62	1.2 ± 0.17	-	0.27
$[\{(bpy)_2Ru(dpp)\}_2RhBr_2](PF_6)_5$	65	TEA	0.62	1.7 ± 0.11	-	0.31
$[\{(phen)_2Ru(dpp)\}_2RhCl_2](PF_6)_5$	65	TEA	0.62	0.99 ± 0.08	-	0.29
$[\{(bpy)_2Ru(dpp)\}_2RhCl_2](PF_6)_5$	65	TEOA	0.62	0.22 ± 0.08	-	0.33
$[\{(bpy)_2Ru(dpp)\}_2RhBr_2](PF_6)_5$	65	TEOA	0.62	0.21 ± 0.05	-	0.37
$[\{(phen)_2Ru(dpp)\}_2RhCl_2](PF_6)_5$	65	TEOA	0.62	0.18 ± 0.03	-	0.35

[a] Final solution concentrations. [b] Final electron donor concentration is 1.5 M. [c] Total hydrogen in the headspace and solution. [d] E_{redox} is the difference between the estimated excited-state reduction potential of the ^{3}MLCT state and the ground-state oxidation potential of the electron donor. All solutions were photolyzed for 2 h using a LED light source. The oxidation potentials of DMA, TEA, and TEOA are 1.05,[47] 1.20,[48] and 1.14 V vs NHE.[49]

hydrogen was assayed in the headspace. All solutions were photolyzed for 2 h in gastight cells using an LED array and experiments were conducted in triplicate. Under these conditions, all light from the LED light source is absorbed and the effective pH with the DMA electron donor is ~9.1, assuming that the pK_a of DMA is similar to that reported in aqueous solutions (pK_a of $DMAH^+ = 5.07$).[36] The large excess of the electron donor dictates the pH of the reaction medium under our conditions. The experiments were performed at two wavelengths for the most effective photocatalysts with three electron donors, as seen in Table 3.

The photocatalysis of water reduction by these supramolecular complexes to produce hydrogen requires first the multielectron reduction of the photocatalyst. Excitation of these complexes produces the $M(d\pi) \rightarrow dpp(\pi^*)$ ^{1}MLCT state, which rapidly intersystem crosses to produce a ^{3}MLCT state. This ^{3}MLCT state can be reductively quenched by an electron donor. The driving force, (E_{redox}), for this reaction depends on the excited-state reduction potential of the photocatalyst ($E(^*CAT^{n+}/CAT^{(n-1)+})$) and the ground-state oxidation potential of the electron donor ($E(ED^{0/+})$), as seen in eqs 4 and 5

$$E_{redox} = E(^*CAT^{n+}/CAT^{(n-1)+}) - E(ED^{0/+}) \quad (4)$$

$$E(^*CAT^{n+}/CAT^{(n-1)+}) = E(CAT^{n+}/CAT^{(n-1)+}) + E^{0-0} \quad (5)$$

where $E(CAT^{n+}/CAT^{(n-1)+})$ is the ground-state reduction potential of the photocatalyst and E^{0-0} is the zero−zero energy of the excited state. E^{0-0} is estimated using the emission energy maxima. Our use of the emission energy provides a low-energy estimate of E^{0-0} and therefore a conservative estimate of E_{redox}. If the electron donor reductively quenches the ^{3}MLCT state of the complex, transfer of the optically promoted electron from the dpp(π^*) orbital to the Rh(dσ^*) orbital should follow, generating a Rh(II) species. The optically excited catalyst can also undergo intramolecular electron transfer of the promoted electron to the Rh(III) acceptor, populating the ^{3}MMCT state, which can then be reductively quenched by the electron donor. Excited-state reduction of the ^{3}MMCT state also affords a Rh(II) species. Multielectron reduction requires this process to occur twice to generate the Rh(I) form of the photocatalyst, for example $[\{(bpy)_2Ru(dpp)\}_2Rh^I]^{5+}$. It is also possible for the Rh(I) complex to further photoreduce under our conditions with additional electrons being localized on the dpp(π^*) orbitals, for example $[\{(bpy)_2Ru(dpp^-)\}_2Rh^I]^{3+}$.

Analysis of the driving forces for the excited-state reductions of the trimetallic complexes by the electron donors provides insight into the expected photocatalysis. An emission quenching analysis has shown that DMA can efficiently quench the emission of the ^{3}MLCT state of $[\{(bpy)_2Ru(dpp)\}_2RhCl_2](PF_6)_5$.[26] The excited-state reduction potentials for the ^{3}MLCT and ^{3}MMCT of $[\{(bpy)_2Ru(dpp)\}_2RhCl_2](PF_6)_5$ have been estimated to be 1.47 and 1.08 V versus NHE, respectively.[26] Thus, DMA ($E_{1/2}^{oxd} = 1.05$ V vs NHE)[47] can thermodynamically reductively quench both the ^{3}MLCT and ^{3}MMCT states of $[\{(bpy)_2Ru(dpp)\}_2RhCl_2](PF_6)_5$. The excited-state properties of the $[\{(bpy)_2Ru(dpp)\}_2RhBr_2](PF_6)_5$ and $[\{(phen)_2Ru(dpp)\}_2RhCl_2](PF_6)_5$ are very similar to those of $[\{(bpy)_2Ru(dpp)\}_2RhCl_2](PF_6)_5$. The excited-state reduction potentials of the ^{3}MLCT and ^{3}MMCT states for $[\{(bpy)_2Ru(dpp)\}_2RhBr_2](PF_6)_5$ are estimated to be 1.51 and 1.12 V versus NHE, and 1.49 and 1.08 V versus NHE for $[\{(phen)_2Ru(dpp)\}_2RhCl_2](PF_6)_5$. These values suggest that the reductive quenching by DMA of $[\{(bpy)_2Ru(dpp)\}_2RhBr_2](PF_6)_5$ or $[\{(phen)_2Ru(dpp)\}_2RhCl_2](PF_6)_5$ should have a similar driving force to that observed for DMA and $[\{(bpy)_2Ru(dpp)\}_2RhCl_2](PF_6)_5$, as is shown in Table 3. Similar to $[\{(bpy)_2Ru(dpp)\}_2RhCl_2](PF_6)_5$, the complexes $[\{(bpy)_2Ru(dpp)\}_2RhBr_2](PF_6)_5$ and $[\{(phen)_2Ru(dpp)\}_2RhCl_2](PF_6)_5$ undergo photoreduction in the presence of DMA in acetonitrile to produce a Rh(I) species, $[\{(TL)_2Ru(dpp)\}_2Rh^I]^{5+}$ (TL = bpy or phen), establishing them as two new photoinitiated electron collectors. The spectroscopic changes associated with the formation of the

(47) Bock, C. R.; Connor, J. A.; Gutierrez, A. R.; Meyer, T. J.; Whitten, D. G.; Sullivan, B. P.; Nagle, J. K. *J. Am. Chem. Soc.* **1979**, *101*, 4815.

(48) Ballardini, R.; Varani, G.; Indelli, M. T.; Scandola, F.; Balzani, V. *J. Am. Chem. Soc.* **1978**, *100*, 7219.

(49) Tazuke, S.; Kitamura, N.; Kim, H.-B. *Photochemical Energy Conversion*; Norris, J. R., Jr., Meisel, D., Eds.; Elsevier: New York, 1989; pp 96−110.

Rh(I) species from $[\{(bpy)_2Ru(dpp)\}_2RhBr_2](PF_6)_5$ and $[\{(phen)_2Ru(dpp)\}_2RhCl_2](PF_6)_5$ are given in the Supporting Information.

The electrochemical, photochemical, and excited-state properties for $[\{(bpy)_2Ru(dpp)\}_2RhCl_2](PF_6)_5$, $[\{(bpy)_2Ru(dpp)\}_2RhBr_2](PF_6)_5$, and $[\{(phen)_2Ru(dpp)\}_2RhCl_2](PF_6)_5$ are very similar predicting similar photocatalytic hydrogen efficiency. The photolysis of $[\{(bpy)_2Ru(dpp)\}_2RhCl_2](PF_6)_5$, $[\{(bpy)_2Ru(dpp)\}_2RhBr_2](PF_6)_5$, and $[\{(phen)_2Ru(dpp)\}_2RhCl_2](PF_6)_5$ with DMA and water at 470 nm affords 6.0, 7.2, and 5.4 μmol of H_2. The ability of all three complexes to photocatalytically produce hydrogen is a significant finding, verifying that our molecular architecture presents a general design for development of future photocatalysts. The ability of $[\{(bpy)_2Ru(dpp)\}_2RhBr_2](PF_6)_5$ to produce larger amounts of hydrogen is indicative of halide being involved in a step that is kinetically important. The greater photocatalytic activity of $[\{(bpy)_2Ru(dpp)\}_2RhBr_2](PF_6)_5$ could be a result of the bromide σ-donor ability modulating electron transfer to produce the ^{3}MMCT state. If such an effect is operative, similar photocatalytic efficiency should be observed for $[\{(phen)_2Ru(dpp)\}_2RhCl_2](PF_6)_5$ as similar k_{et} is observed. Formation of the Rh(I) complex requires halide loss, and the bromide species may facilitate this halide loss, to form the $[\{(bpy)_2Ru(dpp)\}_2Rh^I]^{5+}$ species. Photolysis of $[\{(bpy)_2Ru(dpp)\}_2RhBr_2](PF_6)_5$ with DMA and water in the presence of a 400-fold excess Hg(l) at 470 nm showed no impact on hydrogen production, suggesting decomplexation to form colloidal Rh is not an operating pathway.[24,50] Similar photocatalytic efficiency is observed for $[\{(bpy)_2Ru(dpp)\}_2RhCl_2](PF_6)_5$, $[\{(bpy)_2Ru(dpp)\}_2RhBr_2](PF_6)_5$, and $[\{(phen)_2Ru(dpp)\}_2RhCl_2](PF_6)_5$ (1.9, 1.8, and 2.2 μmol, respectively) when photolysis is conducted by irradiating at 520 nm in the presence of DMA. Photolysis at 520 nm affords lower amounts of hydrogen ($\sim$30%) as compared to photolysis at 470 nm. During photolysis of $[\{(bpy)_2Ru(dpp)\}_2RhCl_2](PF_6)_5$ in the presence of DMA and water, a color change occurs that is characteristic of the shift of the Ru(dπ) $\rightarrow$ dpp(π*) MLCT band from 520 to 460 nm.[27] This shift in the wavelength mirrors the formation of the Rh(I) species, $[\{(TL)_2Ru(dpp)\}_2Rh^I]^{5+}$ (TL = bpy or phen). The lower photocatalytic efficiency when photolysis is performed at 520 nm may be attributed to the decrease in absorbance of the photocatalytic system at 520 nm as the photolysis proceeds. The ability of these three rhodium-based complexes to photocatalytically produce hydrogen from water under basic conditions is significant. The variation of the TL and the coordinated halide does not adversely impact catalyst function. This implies that as long as the supramolecule possesses a Rh(dσ*)-based LUMO and an excited-state with sufficient driving force to oxidize the electron donor, photocatalysis of water reduction to hydrogen will occur.

The complex $[\{(bpy)_2Ru(dpb)\}_2IrCl_2](PF_6)_5$ was analyzed for photochemical hydrogen production from water using the optimized conditions used for $[\{(bpy)_2Ru(dpp)\}_2RhCl_2](PF_6)_5$ in the presence of DMA. The complex was absorbance matched at the wavelength of excitation (470 nm) to $[\{(bpy)_2Ru(dpp)\}_2RhCl_2](PF_6)_5$, which resulted in a concentration of 88 μM. Under these conditions, the iridium complex undergoes facile photoinitiated electron collection.[17] This iridium-based complex did not produce detectable amounts of hydrogen when irradiated at 470 or 520 nm. Unlike the complexes $[\{(bpy)_2Ru(dpp)\}_2RhCl_2](PF_6)_5$, $[\{(bpy)_2Ru(dpp)\}_2RhBr_2](PF_6)_5$, and $[\{(phen)_2Ru(dpp)\}_2RhCl_2](PF_6)_5$, in which photoinitiated electron collection occurs at the rhodium center, photoinitiated electron collection in $[\{(bpy)_2Ru(dpb)\}_2IrCl_2](PF_6)_5$ occurs on the dpb BL. The lack of photochemical hydrogen production using $[\{(bpy)_2Ru(dpb)\}_2IrCl_2](PF_6)_5$ implies that electron collection on the rhodium center is necessary for the photochemical reduction of water and signifies the importance of the rhodium center for hydrogen photocatalysis.

The complexes $[\{(bpy)_2Os(dpp)\}_2RhCl_2](PF_6)_5$, $[\{(tpy)RuCl(dpp)\}_2RhCl_2](PF_6)_3$, and $[\{(tpy)OsCl(dpp)\}_2RhCl_2](PF_6)_3$ were analyzed for photochemical hydrogen production from water using DMA as the electron donor. The complexes $[\{(bpy)_2Os(dpp)\}_2RhCl_2](PF_6)_5$, $[\{(tpy)RuCl(dpp)\}_2RhCl_2](PF_6)_3$, and $[\{(tpy)OsCl(dpp)\}_2RhCl_2](PF_6)_3$ were absorbance matched at the wavelength of excitation (470 nm) to $[\{(bpy)_2Ru(dpp)\}_2RhCl_2](PF_6)_5$, which resulted in concentrations of 50, 118, and 92 μM, respectively. The two complexes $[\{(bpy)_2Os(dpp)\}_2RhCl_2](PF_6)_5$ and $[\{(tpy)RuCl(dpp)\}_2RhCl_2](PF_6)_3$ afford similar amounts of hydrogen (0.13 and 0.21 μmol, respectively) when irradiated at 470 nm, a much lower photocatalytic efficiency relative to $[\{(bpy)_2Ru(dpp)\}_2RhCl_2](PF_6)_5$. The complexes $[\{(bpy)_2Os(dpp)\}_2RhCl_2](PF_6)_5$ and $[\{(tpy)RuCl(dpp)\}_2RhCl_2](PF_6)_3$ do not display detectable emissions. To calculate the excited-state reduction potentials for these complexes, the λ_{max}^{em} for the Os(dπ) $\rightarrow$ dpp(π*) ^{3}MLCT state in $[\{(bpy)_2Os(dpp)\}_2RhCl_2](PF_6)_5$ was estimated to be 930 nm.[43-46] The λ_{max}^{em} from the Ru(dπ) $\rightarrow$ dpp(π*) ^{3}MLCT in $[\{(tpy)RuCl(dpp)\}_2RhCl_2](PF_6)_3$ was estimated to be 820 nm.[43-46] Using these estimates, the excited-state reduction potentials of the ^{3}MLCT and ^{3}MMCT were predicted as 1.15 and 0.78 V for $[\{(bpy)_2Os(dpp)\}_2RhCl_2](PF_6)_5$ and 1.25 and 0.85 V versus NHE for $[\{(tpy)RuCl(dpp)\}_2RhCl_2](PF_6)_3$. These potentials suggest similar driving forces for reductive quenching by suitable electron donors, affording similar photocatalytic efficiency, as is shown in Table 3. Photocatalysis by these complexes implies participation of the ^{3}MLCT excited-state in the observed photolysis as only a small driving force exists for the reductive quenching of only the ^{3}MLCT states. The lower driving force for reductive quenching by DMA and the shorter excited-state lifetimes for these complexes should both lead to lower photocatalytic efficiency relative to $[\{(bpy)_2Ru(dpp)\}_2RhCl_2](PF_6)_5$. The complex $[\{(tpy)OsCl(dpp)\}_2RhCl_2](PF_6)_3$ does not produce detectable hydrogen under the conditions investigated, consistent with the even lower energy of the ^{3}MLCT and ^{3}MMCT states, the shorter expected ^{3}MLCT lifetime relative to $[\{(tpy)RuCl(dpp)\}_2RhCl_2](PF_6)_3$, and the expected slightly negative E_{redox} for the excited-state electron transfer from

(50) (a) Anton, D. R.; Crabtree, R. H. *Organometallics* **1983**, *2*, 855–859. (b) Baba, R.; Nakabayashi, S.; Fujishima, A.; Honda, K. *J. Phys. Chem.* **1985**, *89*, 1902–1905.

DMA. The complexes $[\{(bpy)_2Os(dpp)\}_2RhCl_2](PF_6)_5$, $[\{(tpy)RuCl(dpp)\}_2RhCl_2](PF_6)_3$, and $[\{(tpy)OsCl(dpp)\}_2RhCl_2](PF_6)_3$ do not produce detectable amounts of hydrogen when irradiated at 520 nm for 2 h, likely a reflection of the even lower quantum efficiencies seen at this wavelength.

The three most active photocatalysts, $[\{(bpy)_2Ru(dpp)\}_2RhCl_2](PF_6)_5$, $[\{(bpy)_2Ru(dpp)\}_2RhBr_2](PF_6)_5$, and $[\{(phen)_2Ru(dpp)\}_2RhCl_2](PF_6)_5$, were studied to explore the role of the electron donor on hydrogen photocatalysis. This allows for the variation of the driving force of the excited-state reduction of the photocatalyst. Photolysis of $[\{(bpy)_2Ru(dpp)\}_2RhCl_2](PF_6)_5$, $[\{(bpy)_2Ru(dpp)\}_2RhBr_2](PF_6)_5$, and $[\{(phen)_2Ru(dpp)\}_2RhCl_2](PF_6)_5$ in the presence of the electron donor TEA and water produces hydrogen as expected based on the driving forces for photoreduction. Hydrogen is produced at lower yields using TEA relative to DMA (1.2, 1.7, and 0.99 μmol for $[\{(bpy)_2Ru(dpp)\}_2RhCl_2](PF_6)_5$, $[\{(bpy)_2Ru(dpp)\}_2RhBr_2](PF_6)_5$, and $[\{(phen)_2Ru(dpp)\}_2RhCl_2](PF_6)_5$, respectively). On the basis of the TEA oxidation potential ($E_{1/2}^{ox} = 1.20$ V vs NHE in acetonitrile),[48] a lower driving force for reductive quenching of both the ^{3}MLCT and ^{3}MMCT states relative to DMA is expected, as is shown in Table 3. In addition, DMA may preassociate with $[\{(bpy)_2Ru(dpp)\}_2RhCl_2](PF_6)_5$ through aromatic π-stacking interactions, which can further facilitate reductive quenching and photochemical hydrogen production.[26] The higher effective pH should also impede photocatalytic efficiency when TEA is used as the electron donor. Photolysis of $[\{(bpy)_2Ru(dpp)\}_2RhCl_2](PF_6)_5$, $[\{(bpy)_2Ru(dpp)\}_2RhBr_2](PF_6)_5$, and $[\{(phen)_2Ru(dpp)\}_2RhCl_2](PF_6)_5$ in the presence of the electron donor TEOA and water also produces hydrogen, but at an even lower yield (0.22, 0.21, and 0.18 μmol, for $[\{(bpy)_2Ru(dpp)\}_2RhCl_2](PF_6)_5$, $[\{(bpy)_2Ru(dpp)\}_2RhBr_2](PF_6)_5$, and $[\{(phen)_2Ru(dpp)\}_2RhCl_2](PF_6)_5$, respectively). The oxidation potential of TEOA ($E_{1/2}^{ox} = 1.14$ V vs NHE in acetonitrile)[49] estimates a lower driving force for reductive quenching of both the ^{3}MLCT and ^{3}MMCT states relative to DMA, whereas a slightly larger driving force is estimated relative to TEA. The even lower yield of hydrogen when TEOA is the electron donor relative to TEA and DMA further implies that effective pH of the system and/or aromatic interactions between DMA and the catalyst may greatly impact reductive quenching and photocatalytic efficiency. The greatest photocatalytic efficiency when DMA is the electron donor may be related to changes in the effective pH, which is ca. 9.1 for DMA, 14.7 for TEA, and 11.8 for TEOA. This change in pH may be critical if protonation of a Rh(I) species is important in the photocatalytic pathway. In addition, the reduction potential of water shifts to more negative potentials with increasing pH. Current work focuses on determining the optimized conditions for a variety of electron donors for hydrogen photocatalysis as well as exploring the functioning of these systems in more detail.

Conclusions

The study of the photocatalysis of water reduction by supramolecular catalysts with varying TLs, light absorbing metals, as well as central metals have been described. The complexes selected for assay included the first photochemical molecular device for photoinitiated electron collection, $[\{(bpy)_2Ru(dpb)\}_2IrCl_2](PF_6)_5$, and a series of rhodium centered complexes with Rh(dσ*)-based LUMOs and lowest-lying ^{3}MMCT states. The iridium centered complex is known to photochemically collect electrons to produce the two-electron reduced complex $[\{(bpy)_2Ru(dpb^-)\}_2IrCl_2]^{3+}$ but herein is shown to not produce hydrogen under the photocatalytic conditions. This illustrates the importance of collecting the electrons on a metal center such as rhodium that once reduced to the Rh(I) state forms the coordinately unsaturated square planar complex $[\{(bpy)_2Ru(dpp)\}_2Rh^I]^{5+}$. The role of the coordinated halide was also explored using $[\{(bpy)_2Ru(dpp)\}_2RhBr_2](PF_6)_5$. The bromide complex affords a system with a lower-lying Rh(dσ*) acceptor orbital, providing a larger driving force for intramolecular electron transfer to produce the ^{3}MMCT state. The bromide complex produces hydrogen in higher yield than the originally reported chloride analogue $[\{(bpy)_2Ru(dpp)\}_2RhCl_2](PF_6)_5$. The exploration of the spectroscopic changes upon the photolysis of the bromide complex in the presence of the DMA electron donor establishes this complex as the second photochemical molecular device for electron collection at a metal center in an assembly that remains intact following electron collection. Similarly. we have established that variation of the TL to produce the previously unreported phen complex, $[\{(phen)_2Ru(dpp)\}_2RhCl_2](PF_6)_5$, produces a photochemical molecular device for photoinitiated electron collection at a metal center. The phen analogue functions with very similar efficiency to that of the bpy analogue, providing evidence that TL variation does not significantly alter catalyst functioning, consistent with the lowest-lying ^{3}MLCT state in this structural motif being BL-based. The TL variation can be used to tune the terminal metal dπ orbital energy and thus modulate the excited-state reduction potential of the complex as illustrated through the study of $[\{(tpy)RuCl(dpp)\}_2RhCl_2](PF_6)_3$. This complex functions as a photocatalyst for hydrogen production but with lower quantum efficiency, consistent with the much lower driving force for excited-state reduction by the electron donor. Tuning of the driving force for excited-state reduction is also possible by variation of the terminal metal to Os(II) in place of the previously studied Ru(II). The complex $[\{(bpy)_2Os(dpp)\}_2RhCl_2](PF_6)_5$ also functions as a hydrogen production photocatalyst. Given the much lower driving force for excited-state reduction of this complex by DMA, excited-state reduction of the ^{3}MMCT state of the osmium complex by DMA is not thermodynamically favorable yet this complex produces hydrogen under our conditions. This establishes the ^{3}MLCT state as an important pathway for photoreduction to produce hydrogen. The system with an osmium-based terminal metal and tpy and Cl TLs, $[\{(tpy)OsCl(dpp)\}_2RhCl_2](PF_6)_3$, does not produce hydrogen under our photocatalytic conditions, consistent with the even lower ^{3}MLCT energy in this molecular architecture, prohibiting excited-state reduction. Lower hydrogen production was observed when the driving force for excited-state reduction is lower using the electron donors TEA and TEOA. The study using TEOA provides evidence that driving force for excited-state reduction alone does not provide an explanation for all of the experimental results. The

lower effective pH and possible catalyst−electron donor interaction may provide for the higher hydrogen yield using the DMA electron donor, which is seen for all three most active photocatalysts, $[\{(bpy)_2Ru(dpp)\}_2RhCl_2](PF_6)_5$, $[\{(bpy)_2Ru(dpp)\}_2RhBr_2](PF_6)_5$, and $[\{(phen)_2Ru(dpp)\}_2RhCl_2](PF_6)_5$. The results of the screening of these new photocatalysts reveal that our design for supramolecular complexes as photocatalysts is in fact general and complexes we predicted to function based on basic chemical properties do function and those that we predicted would not function are not photocatalysts. For systems that do function, each new photocatalyst requires optimization of the reaction conditions. Current studies are focused toward the optimization of the conditions, by way of component modification, identifying new electron donors, and identifying optimized conditions for the electron donors. Efforts to extend the supramolecular architecture to couple electron donors are underway.

Acknowledgment. Acknowledgment is made to the Chemical Sciences, Geosciences and Biosciences Division, Office of Basic Energy Sciences, Office of Sciences, U.S. Department of Energy for their generous support of our research. Acknowledgment is also made to the financial collaboration of Phoenix Canada Oil Company, which holds long term license rights to commercialize the technology. The authors thank Dr. Mark Elvington for his assistance.

Supporting Information Available: Cyclic voltammograms, individual electronic absorption spectra for the photocatalysts, and electronic absorption spectral changes during photolysis. This material is available free of charge via the Internet at http://pubs.acs.org.

IC8017387